Functional heterogeneity of IFN-γ–licensed mesenchymal stromal cell immunosuppressive capacity on biomaterials

Brian J. Kwee[a], Johnny Lam[a], Adovi Akue[b], Mark A. KuKuruga[b], Kunyu Zhang[c], Luo Gu[c], and Kyung E. Sung[a,1]

[a]Division of Cellular and Gene Therapies, Office of Tissues and Advanced Therapies, Center for Biologics Evaluation and Research, US Food and Drug Administration, Silver Spring, MD 20993; [b]Office of Vaccines Research and Review, Center for Biologics Evaluation and Research, US Food and Drug Administration, Silver Spring, MD 20993; and [c]Department of Materials Science and Engineering, Institute for NanoBioTechnology, Johns Hopkins University, Baltimore, MD 21218

Edited by Kristi S. Anseth, University of Colorado Boulder, Boulder, CO, and approved July 22, 2021 (received for review March 29, 2021)

Mesenchymal stromal cells (MSCs) are increasingly combined with biomaterials to enhance their therapeutic properties, including their immunosuppressive function. However, clinical trials utilizing MSCs with or without biomaterials have shown limited success, potentially due to their functional heterogeneity across different donors and among different subpopulations of cells. Here, we evaluated the immunosuppressive capacity, as measured by the ability to reduce T-cell proliferation and activation, of interferon-gamma (IFN-γ)–licensed MSCs from multiple donors on fibrin and collagen hydrogels, the two most commonly utilized biomaterials in combination with MSCs in clinical trials worldwide according to *ClinicalTrials.gov*. Variations in the immunosuppressive capacity between IFN-γ–licensed MSC donors on the biomaterials correlated with the magnitude of indoleamine-2,3-dioxygenase activity. Immunosuppressive capacity of the IFN-γ–licensed MSCs depended on the α_V/α_5 integrins when cultured on fibrin and on the α_2/β_1 integrins when cultured on collagen. While all tested MSCs were nearly 100% positive for these integrins, sorted MSCs that expressed higher levels of α_V/α_5 integrins demonstrated greater immunosuppressive capacity with IFN-γ licensing than MSCs that expressed lower levels of these integrins on fibrin. These findings were equivalent for MSCs sorted based on the α_2/β_1 integrins on collagen. These results demonstrate the importance of integrin engagement to IFN-γ licensed MSC immunosuppressive capacity and that IFN-γ–licensed MSC subpopulations of varying immunosuppressive capacity can be identified by the magnitude of integrin expression specific to each biomaterial.

mesenchymal stromal cells | immunosuppression | biomaterials | interferon-gamma

Mesenchymal stromal cells (MSCs) have been shown to be potent regulators and suppressors of immune cells in vitro and in vivo in preclinical animal models (1–5). In particular, MSCs can potently inhibit the proliferation of effector T cells and induce regulatory T-cell differentiation upon stimulation with proinflammatory cytokines, such as tumor necrosis factor alpha (TNF-α) and interferon-gamma (IFN-γ) (4, 5). MSCs have also demonstrated immunosuppressive capacity in vivo in preclinical animal models for a variety of inflammatory and neurodegenerative diseases including graft versus host disease (GvHD) (6), inflammatory bowel diseases (7), and multiple sclerosis (8). Numerous ongoing and completed clinical trials have attempted to utilize the immunoregulatory functions of MSCs for these inflammatory diseases as well as for coronavirus disease 2019 (COVID-19) (3, 9, 10). While there are currently no Food and Drug Administration (FDA)-approved MSC products, some have been approved by regulatory agencies in other jurisdictions, including Alofisel for complex perianal fistulas in Crohn's Disease (TiGenix NV/Takeda, approved in European Union) and Prochymal for GvHD (Osiris Therapeutics Inc./Mesoblast Ltd., approved in Canada and New Zealand) (9). MSCs have thus far shown mixed results in clinical trials for these applications, potentially due to the poor survival and targeting of the cells to the diseased sites and functional heterogeneity of the MSCs (3, 11, 12).

To enhance the regenerative and immunosuppressive capacity of these cells, clinicians and biomedical engineers have sought to enhance the survival, manufacturing efficiency, and delivery of MSCs by combining them with biomaterial scaffolds (13, 14). These scaffolds provide physical support to the cells, as well as adhesion sites for cell surface integrin receptors, which are heterodimers consisting of an α and β subunit (15). By binding to integrin receptors, biomaterials mimic cell-extracellular matrix interactions and can regulate MSC migration, proliferation, survival, and differentiation (16, 17). The majority of published work that combines MSCs with biomaterials has thus far focused on their musculoskeletal differentiation for bone and cartilage tissue engineering applications (14, 18, 19) as well as their ability to indirectly promote wound healing through secretion of regenerative trophic factors (20, 21). Extensive research has also explored the manufacturing of MSCs on biomaterial scaffolds serving as bioreactors (22), with recent work also demonstrating how expansion of MSCs on polyethylene glycol (PEG) hydrogels can enhance their secretome relative to culture on tissue culture polystyrene (TCPS) (23). Furthermore, biomaterials with RGD (tripeptide motif Arginine-Glycine-Aspartate) or collagen binding moieties can regulate and enhance the immunomodulatory role of MSCs (24–26); notably, licensing of MSCs, by exposure to

Significance

Although mesenchymal stromal cell (MSC) therapies, with and without biomaterials, have shown success in preclinical models of inflammatory diseases, they have not shown consistent efficacy in clinical trials for these diseases. This is potentially due to variations in the therapeutic properties of MSCs from different donor patients and amongst different MSC subpopulations. Here, we show that the immunosuppressive function of MSCs stimulated with interferon-gamma depends on specific integrin engagement with the biomaterials they are cultured on. Furthermore, the amount of integrin expression on the cells can predict the magnitude of immunosuppressive function of the MSCs on the biomaterials. This may lead to methods to enrich for MSC subpopulations within each donor that have high immunosuppressive function on biomaterials.

Author contributions: B.J.K., J.L., and K.E.S. designed research; B.J.K., A.A., M.A.K., and K.Z. performed research; K.Z. and L.G. contributed new reagents/analytic tools; B.J.K. analyzed data; and B.J.K. and K.E.S. wrote the paper.

The authors declare no competing interest.

This article is a PNAS Direct Submission.

[1]To whom correspondence may be addressed. Email: kyung.sung@fda.hhs.gov.

This article contains supporting information online at https://www.pnas.org/lookup/suppl/doi:10.1073/pnas.2105972118/-/DCSupplemental.

Published August 26, 2021.

inflammatory cytokines, encapsulated within RGD-modified alginate microgels enhanced allogenic donor cell engraftment relative to licensed, unencapsulated MSCs (25). Interest in these combinations has resulted in at least 54 clinical trials worldwide using MSCs with biomaterials, according to *ClinicalTrials.gov* (*SI Appendix*, Table S1).

The success of clinical trials utilizing MSCs alone or in combination with biomaterials is potentially limited by the inability to reproducibly manufacture functionally equivalent MSCs; this is in part due to intrinsic functional MSC heterogeneity in the form of donor-to-donor variability and intrapopulation heterogeneity of MSCs (27). Furthermore, heterogeneity introduced during the manufacturing of the MSCs, including differences in the initial isolation of the cells, cryopreservation, and cell culture expansion conditions, further adds variability to MSC products (9). Donor-to-donor heterogeneity in MSC immunosuppressive capacity has been explored both in vitro and in vivo and has been shown to correlate with several secreted biological factors (28–30) and cell morphology on TCPS (31). Furthermore, cellular subpopulations within a single donor source of MSCs exhibit varying degrees of immunosuppressive capacity (32, 33), and variations in the presence of these subpopulations have been shown to contribute to donor-to-donor variability (32). Previous work has also explored how to overcome this functional heterogeneity by sorting for subpopulations of MSCs of greater immunoregulatory activity by positivity for the surface marker CD106 (VCAM-1) (33). The majority of work exploring MSC functional heterogeneity, however, has thus far been mainly studied with MSCs cultured in vitro on TCPS and has not explored MSCs cultured on biomaterials, which provide distinct integrin and ligand engagements with cells.

In the present work, we evaluated the immunosuppressive capacity, as measured by the ability to reduce T-cell proliferation and activation, of IFN-γ–licensed human bone marrow–derived MSCs from multiple donors seeded on top of fibrin and collagen hydrogels, the two most commonly utilized biomaterials in combination with MSCs in clinical trials worldwide according to *ClinicalTrials.gov* (*SI Appendix*, Table S1). Immunosuppressive capacity was also studied in the context of indoleamine-2,3-dioxygenase (IDO) activity and programmed death-ligand 1 (PD-L1) expression, key immunomodulatory factors shown to be strongly up-regulated by IFN-γ in human MSCs (34). Furthermore, we evaluated how specific integrin engagement between the cells and the biomaterials, as well as the magnitude of expression of these integrins, influence or predict their immunosuppressive capacity. This work highlights the critical importance of integrin interactions with biomaterials to the immunosuppressive capacity of MSCs and identifies the existence of MSC subpopulations with varying immunosuppressive capacity based on the magnitude of integrin expression specific to a biomaterial. These findings may lead to methods for manufacturing and enriching for highly immunosuppressive MSCs for MSC–biomaterial combination therapies.

Results

Immunosuppressive Capacity of IFN-γ–Licensed MSC Donors on Biomaterials. The immunosuppressive capacity of human bone marrow–derived MSCs from four donors obtained from RoosterBio were first evaluated on fibrin and collagen I hydrogels (Fig. 1). These two hydrogels were normalized to the same weight percent concentration of polymer protein (6 mg/mL) at a concentration that formed stable, solid hydrogels (*SI Appendix*, Table S2). MSCs cultured on these hydrogels were licensed with or without IFN-γ and then cocultured with peripheral blood mononuclear cells (PBMCs), which were stained with carboxyfluorescein succinimidyl ester (CFSE) and activated with anti-CD3/CD28 dynabeads; the PBMCs were then analyzed by flow cytometry. Functional immunosuppressive capacity was measured as the ability of the MSCs to regulate the proliferation and activation of $CD4^+$ and $CD8^+$ T cells in the activated PBMCs as measured by CFSE dilution and CD25 expression, respectively (*SI Appendix*, Fig. S1). Unstimulated MSCs demonstrated varied ability in reducing the proliferation and the activation of the $CD4^+/CD8^+$ T cells both between the various donors and between the two tested hydrogels (Fig. 2 *A–D* and *SI Appendix*, Fig. S2 *A–D*). Licensing with IFN-γ enhanced the ability of the MSCs to reduce the proliferation and, to a lesser extent, the activation of the $CD4^+/CD8^+$ T cells; this enhancement also varied both between the donors and the two tested hydrogels (Fig. 2 *A–D* and *SI Appendix*, Fig. S2 *A–D*). Similar observations were found with unstimulated and IFN-γ–licensed MSCs obtained from AllCells and Lonza cultured on the two hydrogels (*SI Appendix*, Table S3 and Fig. S3). The activity of IDO, an immunosuppressive enzyme that converts tryptophan to kynurenine, and the expression of PD-L1, which binds to PD-1 on T cells to inhibit their activation, were nearly absent in the unlicensed MSCs but

hMSC Donor ID	Sex	Age
RB9	M	43
RB12	M	33
RB14	F	20
RB16	F	29

hydrogels
fibrin (6 mg/mL fibrinogen)
collagen I (6 mg/mL collagen I)

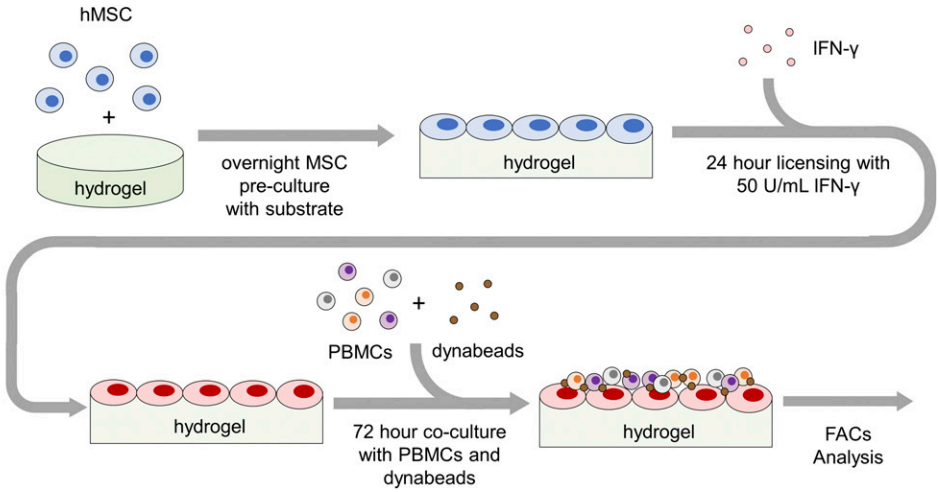

Fig. 1. Evaluating immunosuppressive capacity of IFN-γ–licensed MSCs on hydrogel biomaterials. Experimental setup with (*Upper Left*) list of RoosterBio human bone marrow–derived MSC cell lines tested from various donors, (*Lower Left*) list of tested biomaterial hydrogels, and (*Right*) timeline of experimental procedures. After overnight culture on the biomaterials, the MSC cell lines were licensed with IFN-γ for 24 h and then cocultured with CFSE-stained PBMCs activated with anti-CD3/CD28 dynabeads. After 72 h of coculture, the proliferation and activation of the $CD4^+$ and $CD8^+$ T cells in the PBMCs were measured with flow cytometry analysis.

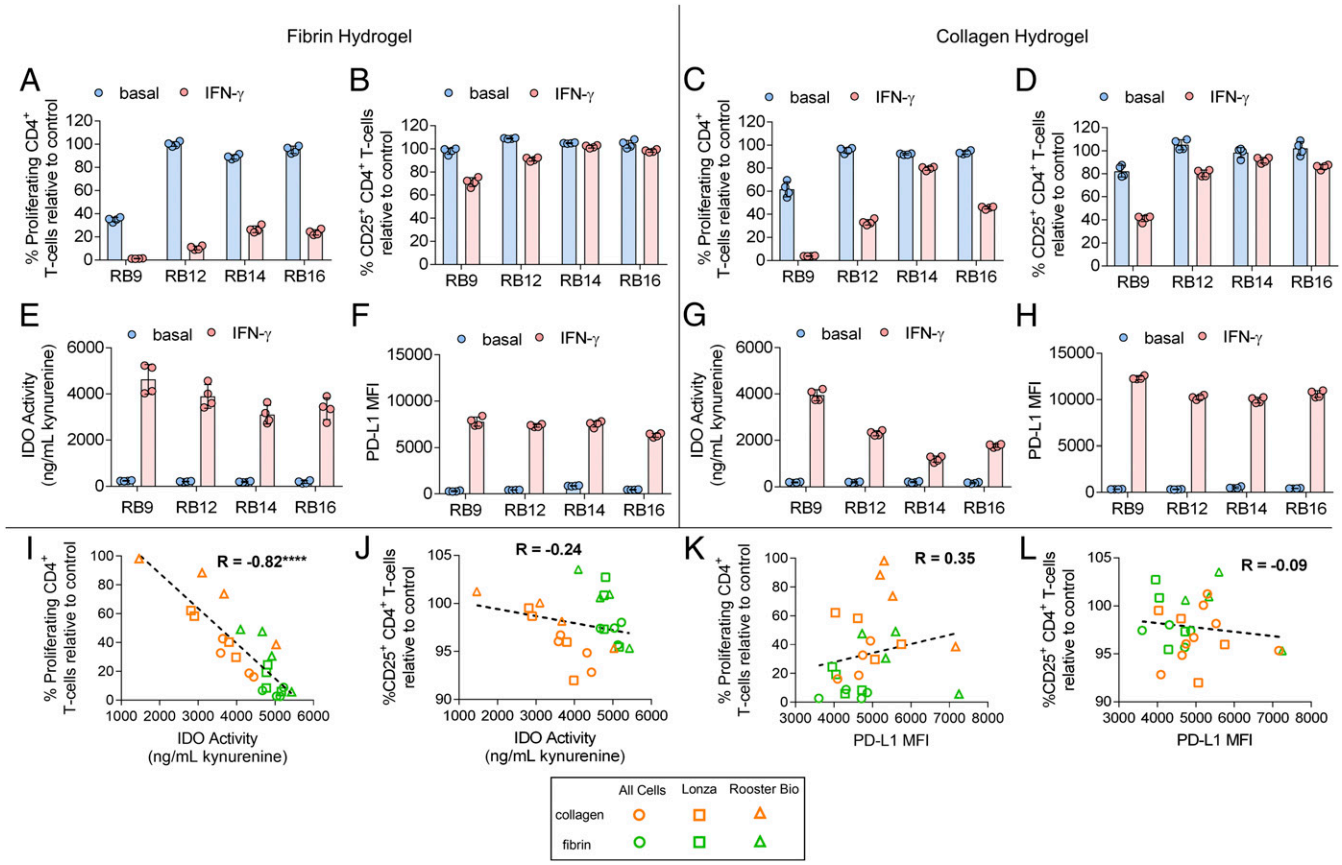

Fig. 2. Immunosuppressive capacity of IFN-γ–licensed MSCs on hydrogel biomaterials. (*A*) The percent of proliferating and (*B*) percent of CD25$^+$ CD4$^+$ T cells in the presence of MSC lines, with and without IFN-γ licensing, cultured on fibrin. (*C*) The percent of proliferating and (*D*) percent of CD25$^+$ CD4$^+$ T cells in the presence of MSC lines, with and without IFN-γ licensing, cultured on collagen. (*E*) Activity of IDO, as measured by concentration of kynurenine in conditioned media, and (*F*) mean fluorescence intensity (MFI) of PD-L1 of various MSC cell lines, with and without IFN-γ licensing, cultured on fibrin. (*G*) Activity of IDO and (*H*) MFI of PD-L1 of various MSC cell lines, with and without IFN-γ licensing, cultured on collagen. (*I* and *J*) Correlation between IDO activity with (*I*) proliferating CD4$^+$ T cells and (*J*) CD25$^+$ CD4$^+$ T cells of IFN-γ–licensed MSC cell lines cultured on fibrin and collagen. (*K* and *L*) Correlation between PD-L1 MFI with (*K*) proliferating CD4$^+$ T-cells and (*L*) CD25$^+$ CD4$^+$ T cells of IFN-γ–licensed MSC cell lines cultured on fibrin and collagen. Data are presented as means ± SD. Significance is denoted by ****$P \leq 0.0001$ by two-tailed Spearman's rank correlation.

strongly up-regulated to different magnitudes in IFN-γ–licensed MSCs between the various donors and between the two tested hydrogels as well (Fig. 2 *E*–*H*).

The role of polymer concentration on the immunosuppressive capacity of the IFN-γ–licensed MSCs on the fibrin and collagen hydrogels was also evaluated with two representative RoosterBio MSC lines. Varying the polymer concentration in both hydrogels resulted in changes in the storage and loss moduli of the hydrogels (*SI Appendix*, Table S2). Changing the fibrinogen concentration in the fibrin hydrogel resulted in moderate or no significant changes in the percent of proliferating and activated CD4$^+$/CD8$^+$ T cells when cocultured with IFN-γ–licensed MSCs (*SI Appendix*, Fig. S4). In contrast, decreasing the collagen I polymer concentration in the collagen hydrogels resulted in a trend of increasing the percent proliferating and/or activated CD4$^+$/CD8$^+$ T cells (thus decreasing immunosuppressive capacity) when cocultured with IFN-γ– licensed MSCs (*SI Appendix*, Fig. S5).

Next, we assessed the relationship between IFN-γ–licensed MSC IDO activity and PD-L1 expression with the proliferation and activation of the cocultured T cells. This was evaluated across 12 different IFN-γ–licensed MSC lines obtained from RoosterBio, AllCells, and Lonza (*SI Appendix*, Table S3). When comparing MSC lines on fibrin and collagen hydrogels together, IDO activity of the IFN-γ–licensed MSC lines significantly correlated with the percent proliferating CD4$^+$/CD8$^+$ T cells but not with the activated CD4$^+$/CD8$^+$ T cells (Fig. 2 *I* and *J*, *SI Appendix*, Fig. S2 *E* and *F*). PD-L1 expression of the IFN-γ–licensed MSC lines did not significantly correlate with either the percent proliferating or activated CD4$^+$/CD8$^+$ T cells (Fig. 2 *K* and *L*, *SI Appendix*, Fig. S2 *G* and *H*). When comparing the MSC cultures on fibrin and collagen separately, however, IDO activity of the IFN-γ–licensed MSC lines significantly correlated with the percent proliferating CD4$^+$/CD8$^+$ T cells and the activated CD4$^+$ T cells (*SI Appendix*, Fig. S6 *A*–*H*). PD-L1 expression did not significantly correlate with the percent proliferating CD4$^+$/CD8$^+$ T cells or activated CD4$^+$ T cells when comparing MSCs cultured on each substrate separately (*SI Appendix*, Fig. S6 *I*–*P*).

To further evaluate the functional importance of IDO activity and PD-L1 expression on IFN-γ–licensed MSC immunosuppressive capacity, an inhibitor to IDO activity [1-methyl-(DL)-tryptophan (1-MT), a competitive IDO inhibitor] and an anti–PD-L1 blocking antibody were added to the IFN-γ–licensed RoosterBio MSCs on fibrin and collagen. The addition of an antibody against PD-L1 binding to the IFN-γ–licensed MSC lines had a moderate or no significant effect on the percent proliferating or activated CD4$^+$/CD8$^+$ T cells for the MSC lines cultured on fibrin and collagen (Fig. 3 *A*–*D*, *SI Appendix*, Fig. S7 *A*–*D*). In contrast, addition of 1-MT to the IFN-γ–licensed MSC lines significantly

increased the percent proliferating and activated $CD4^+$ T cells for all the MSC lines on both fibrin and collagen (Fig. 3 *A–D*). For $CD8^+$ T cells, addition of 1-MT to the IFN-γ–licensed MSC lines significantly increased the proliferating and activated T cells for all the MSC lines on fibrin and for at least half of the MSC lines on collagen (*SI Appendix*, Fig. S7 *A–D*).

IFN-γ–Licensed MSC Immunosuppressive Capacity on Biomaterials Depends on Integrin Engagement. The role of specific integrin interactions with the hydrogel biomaterials on the immunosuppressive capacity of the four IFN-γ–licensed RoosterBio MSCs was then tested. For MSCs cultured on fibrin, the role of the RGD integrin subunits α_V and α_5 was evaluated by adding binding inhibitors to each integrin subunit. Addition of an α_V inhibitor alone to the IFN-γ–licensed MSC lines had a moderate or no significant effect on the percent proliferating and activated $CD4^+/CD8^+$ T cells for all the MSC lines (Fig. 4 *A* and *B*, *SI Appendix*, Fig. S8 *A* and *B*). Inhibiting the α_5 subunit alone significantly increased the percent proliferating $CD4^+/CD8^+$ T cells for three of the MSC lines (Fig. 4*A*, *SI Appendix*, Fig. S8*A*). Furthermore, the addition of an α_5 inhibitor alone significantly enhanced the activated $CD4^+/CD8^+$ T cells for two of the MSC lines (Fig. 4*B*, *SI Appendix*, Fig. S8*B*). Strikingly, inhibiting binding of both the α_V and the α_5 integrin subunits in the IFN-γ–licensed MSCs significantly increased the percent proliferating $CD4^+/CD8^+$ T cells for all the MSC cell lines (Fig. 4*A*, *SI Appendix*, Fig. S8*A*); inhibiting both integrin subunits also significantly increased the percent proliferating $CD4^+/CD8^+$ T cells relative to inhibiting the α_5 subunit alone (Fig. 4*A*, *SI Appendix*, Fig. S8*A*). The presence of both the α_V and the α_5 inhibitor to the IFN-γ–licensed MSCs also significantly increased the percent activated $CD4^+/CD8^+$ T cells for three of the MSC lines (Fig. 4*B*, *SI Appendix*, Fig. S8*B*). Addition of an isotype control antibody for the respective integrin blocking antibodies to the IFN-γ–licensed MSCs did not significantly increase the percent proliferating and activated $CD4^+/CD8^+$ T cells for all the MSC lines on fibrin (*SI Appendix*, Fig. S9 *A–D*).

The role of binding of the α_V and α_5 RGD integrin subunits on IDO activity, PD-L1 expression, and cell spreading in the IFN-γ–licensed RoosterBio MSCs cultured on fibrin was also evaluated. The addition of the α_V inhibitor alone or the α_5 inhibitor alone to the IFN-γ– licensed MSCs had no significant effect on IDO activity (Fig. 4*C*). However, the presence of both the α_V and the α_5 inhibitors significantly decreased IDO activity for all the MSC lines (Fig. 4*C*). Addition of the α_V inhibitor alone or the α_5 inhibitor alone to the IFN-γ–licensed MSCs moderately but significantly reduced PD-L1 expression in two of the MSC lines (Fig. 4*D*). The combination of the α_V inhibitor and the α_5 inhibitor had a synergistic effect and significantly decreased PD-L1 expression in all the MSC lines (Fig. 4*D*). In two representative RoosterBio MSC lines, the addition of the α_V inhibitor alone, the α_5 inhibitor alone, or a respective isotype control antibody to the IFN-γ–licensed MSCs had no observable effect on cell spreading (*SI Appendix*, Fig. S10). However, the presence of both the α_V and the α_5 inhibitors reduced cell spreading in the IFN-γ–licensed MSCs (*SI Appendix*, Fig. S10).

For MSCs cultured on collagen, the role of the collagen integrin subunits α_2 and β_1 was evaluated by adding binding inhibitors to each integrin subunit to the IFN-γ–licensed RoosterBio MSCs. Addition of the α_2 inhibitor alone to the IFN-γ–licensed MSC lines significantly increased the percent proliferating $CD4^+$ T cells for all the MSC lines and the percent of proliferating $CD8^+$ T cells for three of the MSC lines (Fig. 5*A*, *SI Appendix*, Fig. S11*A*). The inhibition of β_1 integrin binding alone significantly increased the percent of proliferating $CD4^+$ T cells for all the MSC lines and the percent proliferating $CD8^+$ T cells for two of the MSC lines (Fig. 5*A*, *SI Appendix*, Fig. S11*A*). The presence of both the α_2 inhibitor and the β_1 inhibitor to the IFN-γ–licensed MSC lines significantly increased the percent of

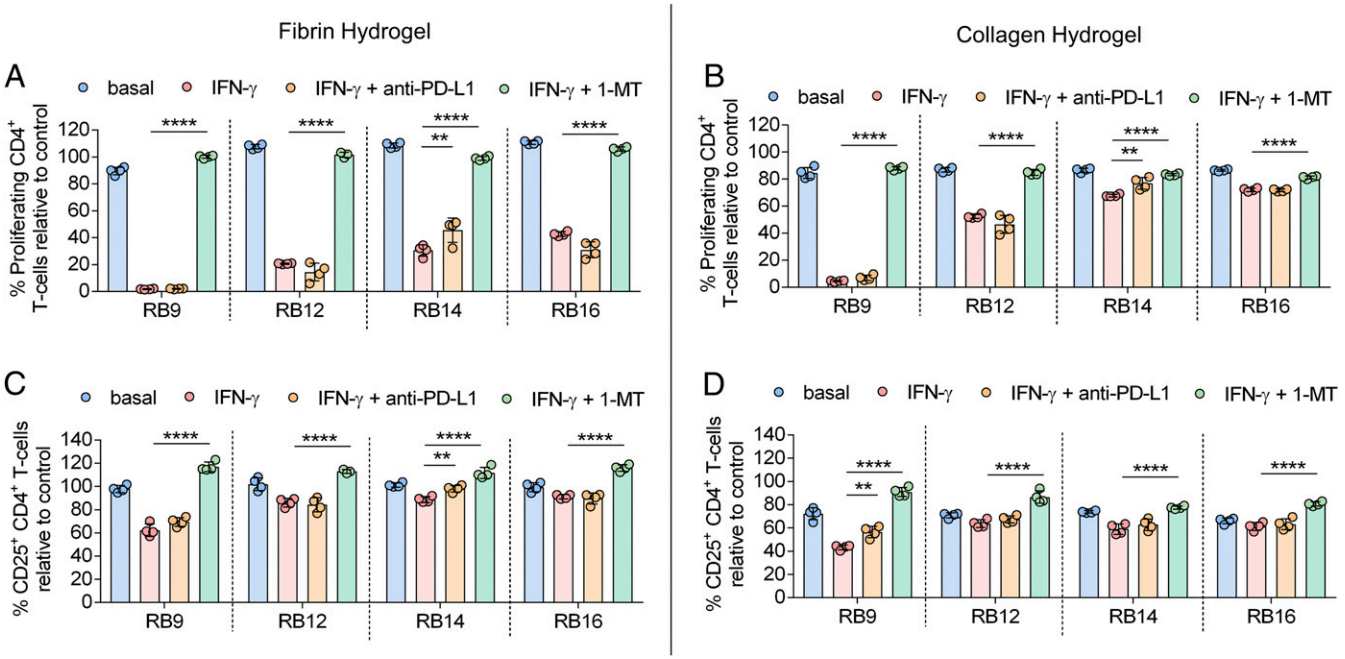

Fig. 3. IDO activity strongly regulates functional immunosuppressive capacity of IFN-γ–licensed MSCs on hydrogel biomaterials. (*A* and *B*) The percent proliferating $CD4^+$ T cells in the presence of MSC lines, with and without IFN-γ licensing, cultured on (*A*) fibrin or (*B*) collagen with and without the addition of anti–PD-L1 antibody or 1-MT, an IDO inhibitor. (*C* and *D*) The percent of $CD25^+$ $CD4^+$ T cells in the presence of MSC lines, with and without IFN-γ licensing, cultured on (*C*) fibrin or (*D*) collagen with and without the addition of anti–PD-L1 antibody or 1-MT. $n = 3$ to 4 for all data sets. Data are presented as means ± SD. Significance is denoted by $^{**}P \leq 0.01$ or $^{****}P \leq 0.0001$ by one-way ANOVA with Tukey's post hoc test; separate comparisons were made between conditions of each cell line.

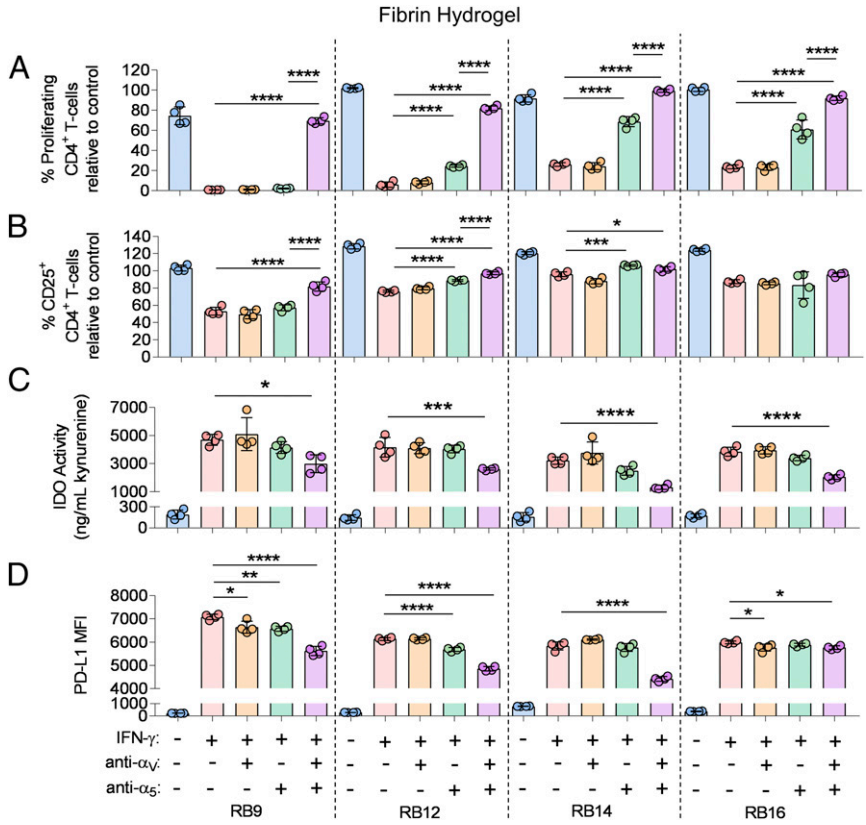

Fig. 4. Engagement of α_V and α_5 integrin subunits regulates immunosuppressive capacity of IFN-γ–licensed MSCs on fibrin hydrogels. (*A*) The percent proliferating and (*B*) $CD25^+$ $CD4^+$ T cells in the presence of various MSCs lines, with and without IFN-γ licensing, cultured on fibrin, with and without the addition of inhibitors to α_V and/or α_5 integrin binding. (*C*) Activity of IDO and (*D*) mean fluorescence intensity (MFI) of PD-L1 of various MSC cell lines, with and without IFN-γ licensing, cultured on fibrin, with and without the addition of inhibitors to α_V and/or α_5 integrin binding. Labels for groups in *A–D* are shown in *D*. $n = 4$ for all data sets. Data are presented as means ± SD. Significance is denoted by $^*P \leq 0.05$, $^{**}P \leq 0.01$, $^{***}P \leq 0.001$, or $^{****}P \leq 0.0001$ by one-way ANOVA with Tukey's post hoc test; separate comparisons were made between conditions of each cell line.

proliferating $CD4^+$ T cells for three of the MSC lines and the percent of proliferating $CD8^+$ T cells for two of the MSC lines (Fig. 5*A*, *SI Appendix*, Fig. S11*A*). In terms of regulating T-cell activation, the α_2 inhibitor alone did not significantly increase the activated $CD4^+/CD8^+$ T cells for the IFN-γ–licensed MSC lines (Fig. 5*B*, *SI Appendix*, Fig. S11*B*). Strikingly, the addition of the β_1 integrin inhibitor alone or both the α_2 and β_1 inhibitors to the IFN-γ–licensed MSCs significantly increased the percent of activated $CD4^+/CD8^+$ T cells to the same extent for all MSC lines (Fig. 5*B*, *SI Appendix*, Fig. S11*B*). The isotype control antibody for the respective integrin blocking antibodies did not significantly increase the percent proliferating and activated $CD4^+/CD8^+$ T cells for the MSC lines on collagen (*SI Appendix*, Fig. S12 *A–D*).

The role of binding of the α_2 and β_1 collagen integrin subunits on IDO activity, PD-L1 expression, and cell spreading of the IFN-γ–licensed RoosterBio MSCs was also determined. The addition of the α_2 inhibitor alone to the IFN-γ–licensed MSCs significantly decreased IDO activity in one MSC line (Fig. 5*C*). The presence of the β_1 integrin inhibitor alone or both the α_2 and the β_1 inhibitors to the IFN-γ–licensed MSCs significantly decreased IDO activity across all the MSC lines to the same extent (Fig. 5*C*). Addition of the α_2 inhibitor alone, β_1 inhibitor alone, or both inhibitors significantly decreased PD-L1 expression in all the MSC lines (Fig. 5*D*). The β_1 inhibitor alone and presence of both inhibitors decreased PD-L1 expression to the greatest extent (Fig. 5*D*). In two representative RoosterBio MSC lines, the addition of the α_2 inhibitor alone and the respective isotype control antibody to the IFN-γ–licensed MSCs had no observable effect on cell spreading (*SI Appendix*, Fig. S13). The presence of the β_1 inhibitor alone reduced cell spreading, while the addition of both the α_2 inhibitor and the β_1 inhibitor further reduced cell spreading in the IFN-γ–licensed MSCs (*SI Appendix*, Fig. S13).

For MSCs cultured on TCPS, the role of the α_V and α_5 RGD integrin subunits on the immunosuppressive capacity and cell spreading of two representative IFN-γ–licensed RoosterBio MSC lines was evaluated. Addition of an α_V inhibitor alone to the IFN-γ–licensed MSC lines significantly increased the percent proliferating and activated $CD4^+/CD8^+$ T cells for both MSC lines (*SI Appendix*, Fig. S14). Addition of the α_5 inhibitor alone had no significant effect in increasing the percent proliferating or activated $CD4^+/CD8^+$ T cells relative to the respective Rat IgG2a isotype control for both MSC lines (*SI Appendix*, Fig. S14). Inhibiting binding of both the α_V and the α_5 integrin subunits in the IFN-γ–licensed MSCs significantly increased the percent proliferating and activated $CD4^+$ T cells relative to the α_V inhibitor alone condition for one of the MSC cell lines (*SI Appendix*, Fig. S14). Similarly, the presence of the α_V inhibitor alone decreased the cell spreading of the IFN-γ–licensed MSCs (*SI Appendix*, Fig. S15). In one of the MSC cell lines, the combined presence of both the α_V and α_5 integrin inhibitors further decreased the cell spreading of the IFN-γ–licensed MSCs relative to the α_V inhibitor alone condition (*SI Appendix*, Fig. S15).

The Role of the Magnitude of Integrin Expression on Functional Heterogeneity of IFN-γ–Licensed MSC Immunosuppressive Capacity. The role of integrin expression on donor-to-donor variations in

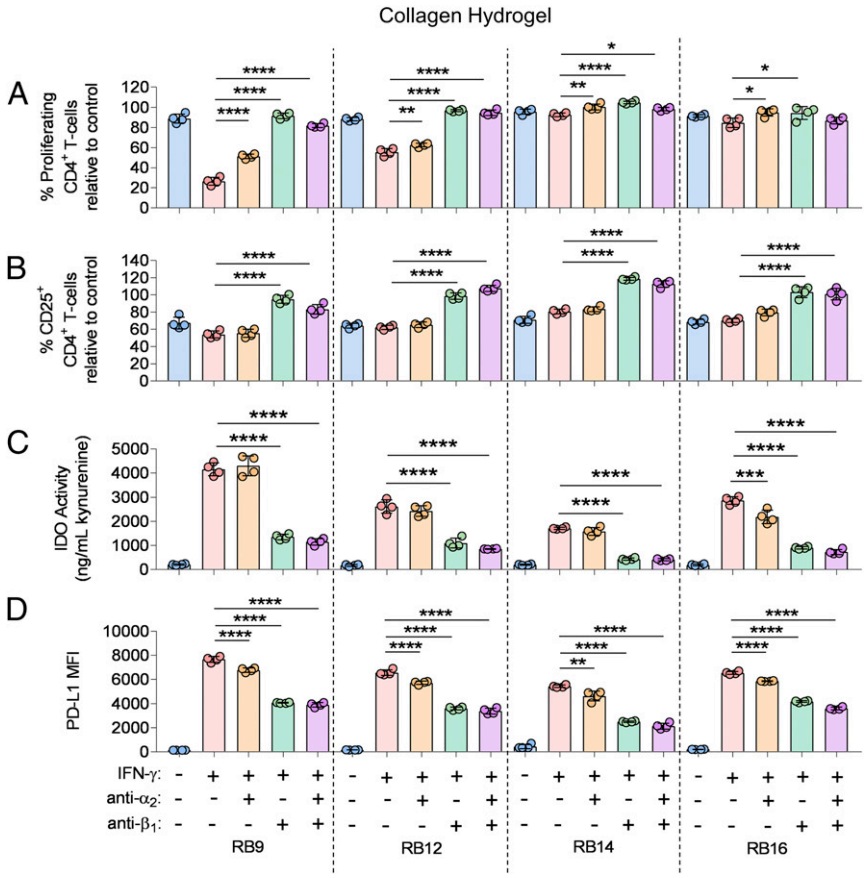

Fig. 5. Engagement of α_2 and β_1 integrin subunits regulates immunosuppressive capacity of IFN-γ–licensed MSCs on collagen hydrogels. (*A*) The percent proliferating and (*B*) $CD25^+$ $CD4^+$ T cells in the presence of various MSCs lines, with and without IFN-γ licensing, cultured on collagen, with and without the addition of inhibitors to α_2 and/or β_1 integrin binding. (*C*) Activity of IDO and (*D*) mean fluorescence intensity (MFI) of PD-L1 of various MSC cell lines, with and without IFN-γ licensing, cultured on collagen, with and without the addition of inhibitors to α_2 and/or β_1 integrin binding. Labels for groups in *A–D* are shown in *D*. $n = 4$ for all data sets. Data are presented as means ± SD. Significance is denoted by $^*P \leq 0.05$, $^{**}P \leq 0.01$, $^{***}P \leq 0.001$, or $^{****}P \leq 0.0001$ by one-way ANOVA with Tukey's post hoc test; separate comparisons were made between conditions of each cell line.

IFN-γ–licensed MSC immunosuppressive capacity was then explored. The expression of the RGD and collagen integrin subunits that contributed to IFN-γ–licensed immunosuppressive capacity on fibrin and collagen were found to be >99% positive for α_V, >96% positive for α_5, >99% positive for α_2, and 100% positive for β_1 on the 12 tested, unlicensed MSC cell lines from RoosterBio, AllCells, or Lonza (*SI Appendix*, Fig. S16). Furthermore, the magnitude of expression of these integrin subunits, as measured by fluorescence intensity in flow cytometry analysis, varied between the tested MSC lines (*SI Appendix*, Fig. S16). Correlations between the immunosuppressive capacity of the various IFN-γ–licensed MSCs donors on fibrin or collagen with the magnitude of the corresponding integrin expression were then evaluated. For MSCs cultured on fibrin, the magnitude of α_V and α_5 integrin expression did not significantly correlate with the percent proliferating or activated $CD4^+/CD8^+$ T cells of the IFN-γ–licensed MSCs as well as the magnitude of IDO activity (*SI Appendix*, Fig. S17). Interestingly, the magnitude of α_V, but not α_5 integrin expression, correlated with the magnitude of PD-L1 expression (*SI Appendix*, Fig. S17 *U* and *V*). For MSCs cultured on collagen, the magnitude of α_2 and β_1 integrin expression did not significantly correlate with the percent proliferating or activated $CD4^+/CD8^+$ T cells of the IFN-γ–licensed MSCs as well as the magnitude of IDO activity and PD-L1 expression (*SI Appendix*, Fig. S17).

Given that all tested MSCs were >96% positive for the RGD integrin subunits α_V and α_5, the role of the magnitude of RGD integrin expression on the immunosuppressive capacity of IFN-γ– licensed MSC subpopulations within each donor on fibrin was then explored. To evaluate this, unlicensed RoosterBio MSCs were fluorescently stained for the α_V/α_5 integrins and sorted by fluorescence-activated cell sorting (FACS) into $\alpha_V^{LO}\alpha_5^{LO}$, $\alpha_V^{MED}\alpha_5^{MED}$, and $\alpha_V^{HI}\alpha_5^{HI}$ MSC subpopulations (Fig. 6*B* and *SI Appendix*, Fig. S18). These sorted MSCs were compared against unsorted MSCs that were either unstained or stained with the same FACS antibodies to evaluate any negative impact of antibody binding to the integrins. All sorted and unsorted, unlicensed MSCs were subsequently cultured on fibrin and licensed with IFN-γ. The $\alpha_V^{MED}\alpha_5^{MED}$ subpopulation significantly reduced the proliferation of the $CD4^+$ T cells to a greater extent than the $\alpha_V^{LO}\alpha_5^{LO}$ MSCs for all the MSC cell lines (Fig. 6*C*). The $\alpha_V^{HI}\alpha_5^{HI}$ subpopulation significantly reduced the proliferation of the $CD4^+$ T cells relative to the $\alpha_V^{LO}\alpha_5^{LO}$, $\alpha_V^{MED}\alpha_5^{MED}$ and unsorted, stained MSCs for all the MSC cell lines (Fig. 6C). For $CD8^+$ T cells, the $\alpha_V^{HI}\alpha_5^{HI}$ subpopulation significantly reduced the proliferation of the T cells relative to the $\alpha_V^{LO}\alpha_5^{LO}$ and unsorted, stained MSCs for all MSC lines and relative to the $\alpha_V^{MED}\alpha_5^{MED}$ cells for two of the MSC lines (*SI Appendix*, Fig. S19*A*). Furthermore, the unstained, unsorted MSCs reduced the proliferation of the $CD4^+/CD8^+$ T cells to a greater extent than the stained, unsorted MSCs for three of the MSC lines (Fig. 6*C*, *SI Appendix*, Fig. S19*A*). These trends were observed to a lesser extent in terms of reducing the activation of T cells. The $\alpha_V^{HI}\alpha_5^{HI}$ subpopulation significantly reduced the activation of $CD4^+$ T cells relative to the $\alpha_V^{LO}\alpha_5^{LO}$ and unsorted, stained MSCs for two of

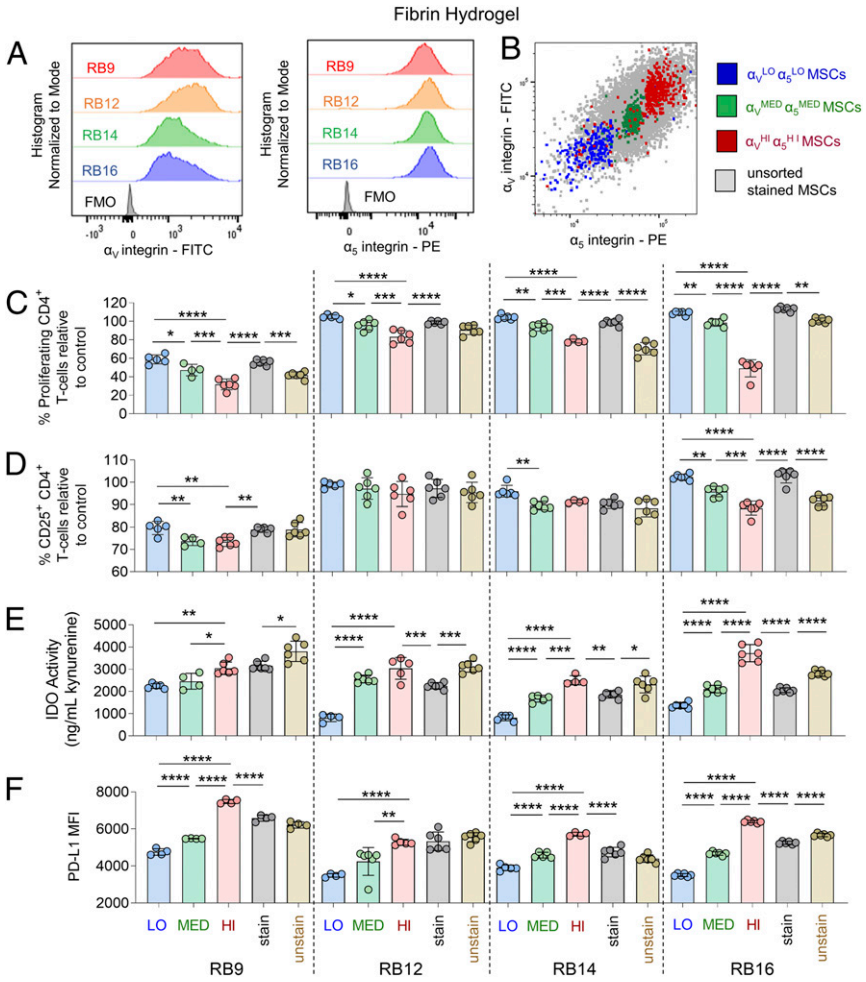

Fig. 6. Magnitude of α_V and α_5 integrin subunits identifies MSC subpopulations of varying immunosuppressive capacity with IFN-γ licensing on fibrin hydrogels. (*A*) FACS plots of α_V expression (*Left*) and α_5 expression (*Right*) of various MSC cell lines. (*B*) Representative FACS plot of FACS-sorted $\alpha_V^{LO}\alpha_5^{LO}$-expressing MSCs, $\alpha_V^{MED}\alpha_5^{MED}$-expressing MSCs, and $\alpha_V^{HI}\alpha_5^{HI}$-expressing MSCs and unsorted MSCs. (*C*) The percent proliferating and (*D*) $CD25^+$ $CD4^+$ T cells in the presence of FACS-sorted or unsorted MSCs lines with IFN-γ licensing, cultured on fibrin. (*E*) Activity of IDO and (*F*) mean fluorescence intensity (MFI) of PD-L1 of FACS-sorted or unsorted MSCs lines with IFN-γ licensing, cultured on fibrin. Labels for groups in *C*–*F* are shown in *F*, where "LO" denotes $\alpha_V^{LO}\alpha_5^{LO}$-expressing MSCs, "MED" denotes $\alpha_V^{MED}\alpha_5^{MED}$-expressing MSCs, "HI" denotes $\alpha_V^{HI}\alpha_5^{HI}$-expressing MSCs, "stain" denotes unsorted MSCs stained with FACS-sorting antibodies, and "unstain" denotes unsorted, unstained MSCs. $n = 4$ to 6 for all data sets. Data are presented as means ± SD. Significance is denoted by $^*P \le 0.05$, $^{**}P \le 0.01$, $^{***}P \le 0.001$, or $^{****}P \le 0.0001$ by one-way ANOVA with Tukey's post hoc test; separate comparisons were made between conditions of each cell line.

the MSC lines (Fig. 6*D*). For $CD8^+$ T cells, these trends were observed significantly for three of the MSC lines (*SI Appendix*, Fig. S19*B*). Unstained, unsorted MSCs reduced the activation of the $CD4^+$ T cells relative to the stained, unsorted MSCs for one of the MSC lines and for all the MSC lines in terms of $CD8^+$ T cells (Fig. 6*D*, *SI Appendix*, Fig. S19*B*). Overall similar observations were obtained with a representative MSC line obtained from AllCells (BM2893) and a representative MSC line from Lonza (1F3422) sorted by FACS into $\alpha_V^{LO}\alpha_5^{LO}$, $\alpha_V^{MED}\alpha_5^{MED}$, and $\alpha_V^{HI}\alpha_5^{HI}$ MSC subpopulations (*SI Appendix*, Fig. S20).

The magnitude of RGD integrin expression in unlicensed MSCs was also found to be associated with the magnitude of IDO activity and PD-L1 expression in subpopulations of IFN-γ–licensed MSCs. In three of the RoosterBio MSC lines, the $\alpha_V^{MED}\alpha_5^{MED}$ subpopulation had significantly greater IDO activity relative to the $\alpha_V^{LO}\alpha_5^{LO}$ MSCs (Fig. 6*E*). Furthermore, the $\alpha_V^{HI}\alpha_5^{HI}$ subpopulation had significantly greater IDO activity relative to the $\alpha_V^{MED}\alpha_5^{MED}$ and unsorted, stained MSCs for three of the MSC lines and relative to the $\alpha_V^{LO}\alpha_5^{LO}$ for all the MSC lines (Fig. 6*E*). The unsorted, stained MSCs had significantly less IDO activity than the unsorted, unstained MSCs for all the MSC lines (Fig. 6*E*). These observed trends were largely similar for PD-L1 expression, as the $\alpha_V^{MED}\alpha_5^{MED}$ subpopulation had significantly greater PD-L1 expression relative to the $\alpha_V^{LO}\alpha_5^{LO}$ MSCs for three of the MSC lines (Fig. 6*F*). Also, the $\alpha_V^{HI}\alpha_5^{HI}$ subpopulation had significantly greater PD-L1 expression relative to the $\alpha_V^{LO}\alpha_5^{LO}$, $\alpha_V^{MED}\alpha_5^{MED}$, and unsorted, stained MSCs for all the MSC lines (Fig. 6*F*). However, the unsorted, stained MSC lines had significantly less PD-L1 expression relative to unsorted, unstained MSCs for only one of the MSC lines (Fig. 6*F*).

The role of the magnitude of RGD integrin expression on the immunosuppressive capacity of IFN-γ–licensed MSC subpopulations on TCPS was also explored with two representative RoosterBio MSC lines. Unlicensed RoosterBio MSCs were similarly fluorescently stained and sorted by FACS into $\alpha_V^{LO}\alpha_5^{LO}$, $\alpha_V^{MED}\alpha_5^{MED}$, and $\alpha_V^{HI}\alpha_5^{HI}$ MSC subpopulations and compared against unsorted, stained and unsorted, unstained MSCs. Following IFN-γ licensing on TCPS, the $\alpha_V^{HI}\alpha_5^{HI}$ subpopulation significantly reduced the proliferation of the $CD4^+$/$CD8^+$ T cells and the activation of the $CD4^+$/ $CD8^+$ T cells relative to the

$\alpha_V^{LO}\alpha_5^{LO}$, $\alpha_V^{MED}\alpha_5^{MED}$, and unsorted, stained MSCs for both MSC cell lines (*SI Appendix*, Fig. S21) Furthermore, the unsorted, unstained MSCs reduced the proliferation of the $CD4^+/CD8^+$ T cells and the activation of the $CD4^+$ T cells to a greater extent than the unsorted, stained MSCs for one of the MSC lines (*SI Appendix*, Fig. S21).

Given that all tested MSC lines were also >99% positive for the collagen integrin subunits α_2 and β_1, the role of the magnitude of these collagen integrins on the immunosuppressive capacity of IFN-γ–licensed MSC subpopulations on collagen was also explored. Unlicensed RoosterBio MSCs were similarly FACS sorted in $\alpha_2^{LO}\beta_1^{LO}$, $\alpha_2^{MED}\beta_1^{MED}$, and $\alpha_2^{HI}\beta_1^{HI}$ MSC subpopulations (Fig. 7*B*, *SI Appendix*, Fig. S22) and compared to unsorted, stained and unsorted, unstained MSCs. Following IFN-γ licensing on collagen, the $\alpha_2^{HI}\beta_1^{HI}$ subpopulation had significantly lower $CD4^+/CD8^+$ T-cell proliferation relative to the $\alpha_2^{LO}\beta_1^{LO}$, $\alpha_2^{MED}\beta_1^{MED}$, and unsorted, stained MSCs for the majority of the MSC lines (Fig. 7*C*, *SI Appendix*, Fig. S23*A*). These trends were observed to a lesser extent in terms of reducing T-cell activation, as the $\alpha_2^{MED}\beta_1^{MED}$ subpopulation significantly reduced the activated $CD4^+$ T cells relative to the $\alpha_2^{LO}\beta_1^{LO}$ MSCs for half the MSC lines (Fig. 7*D*). Furthermore, the $\alpha_2^{HI}\beta_1^{HI}$ subpopulation significantly reduced the activated $CD4^+/CD8^+$ T cells relative to the $\alpha_2^{MED}\beta_1^{MED}$ MSCs for half of the MSC lines (Fig. 7*D*, *SI Appendix*, Fig. S23*B*). The unsorted, stained MSC lines had significantly greater proliferating and activated $CD4^+/CD8^+$ T cells relative to the unsorted, unstained MSCs for only one of the MSC lines (Fig. 7 *C* and *D*, *SI Appendix*, Fig. S23). Overall similar observations were obtained with a representative MSC line obtained from AllCells (BM2893) and a representative MSC line from Lonza (1F3422) sorted by FACS into $\alpha_2^{LO}\beta_1^{LO}$, $\alpha_2^{MED}\beta_1^{MED}$, and $\alpha_2^{HI}\beta_1^{HI}$ MSC subpopulations (*SI Appendix*, Fig. S24).

The magnitude of collagen integrin expression in unlicensed MSCs similarly predicted the magnitude of IDO activity and PD-L1 expression in subpopulations of IFN-γ–licensed MSCs. In two of the RoosterBio MSC lines, the $\alpha_2^{MED}\beta_1^{MED}$ subpopulation had significantly greater IDO activity relative to the $\alpha_2^{LO}\beta_1^{LO}$ MSCs (Fig. 7*E*). Furthermore, the $\alpha_2^{HI}\beta_1^{HI}$ subpopulation had significantly greater IDO activity relative to the unsorted, stained MSCs for three of the MSC lines and relative to the $\alpha_V^{LO}\alpha_5^{LO}$

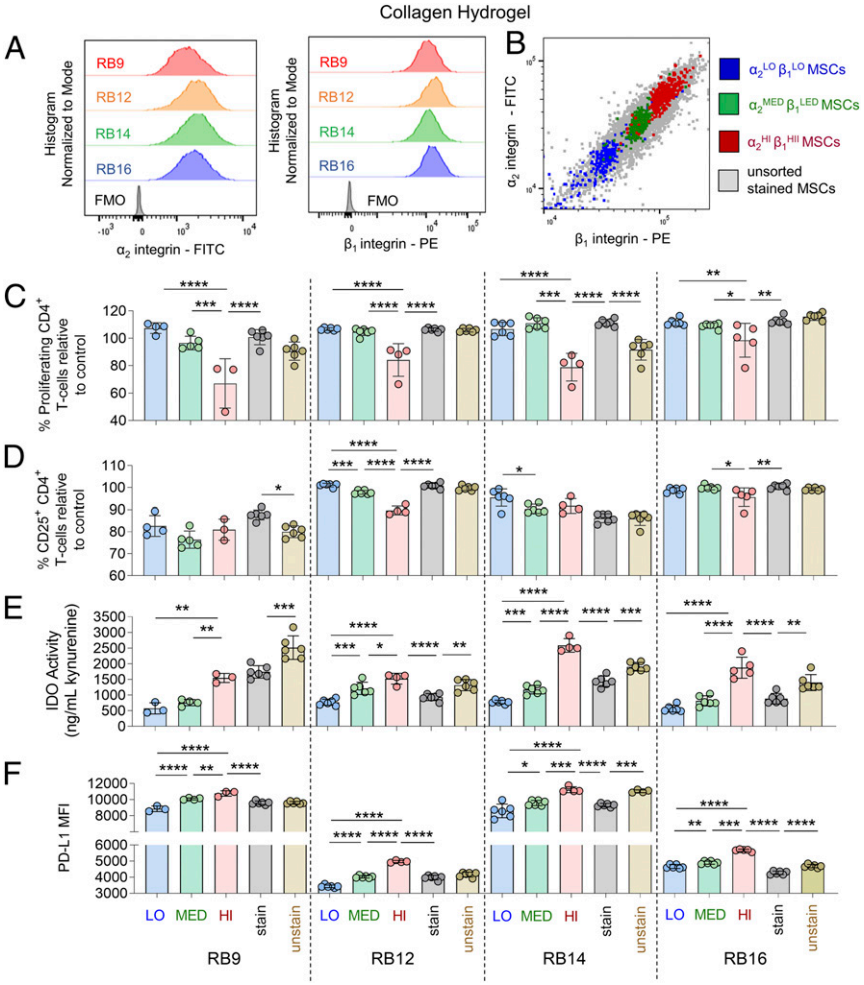

Fig. 7. Magnitude of α_2 and β_1 integrin subunits identifies MSC subpopulations of varying immunosuppressive capacity with IFN-γ licensing on collagen hydrogels. (*A*) FACS plots of α_2 expression (*Left*) and β_1 expression (*Right*) of various MSC cell lines. (*B*) Representative FACS-sorting plot of FACs-sorted $\alpha_2^{LO}\beta_1^{LO}$-expressing MSCs, $\alpha_2^{MED}\beta_1^{MED}$-expressing MSCs, and $\alpha_2^{HI}\beta_1^{HI}$-expressing MSCs with unsorted MSCs. (*C*) The percent proliferating and (*D*) $CD25^+$ $CD4^+$ T cells in the presence of FACS-sorted or unsorted MSCs lines with IFN-γ licensing, cultured on collagen. (*E*) Activity of IDO and (*F*) mean fluorescence intensity (MFI) of PD-L1 of FACS-sorted or unsorted MSCs lines with IFN-γ licensing, cultured on collagen. Labels for groups in *C*–*F* are shown in *F*, where "LO" denotes $\alpha_2^{LO}\beta_1^{LO}$-expressing MSCs, "MED" denotes $\alpha_2^{MED}\beta_1^{MED}$-expressing MSCs, "HI" denotes $\alpha_2^{HI}\beta_1^{HI}$-expressing MSCs, "stain" denotes unsorted MSCs stained with FACS-sorting antibodies, and "unstain" denotes unsorted, unstained MSCs. $n = 3$ to 6 for all data sets. Data are presented as means ± SD. Significance is denoted by $^*P \le 0.05$, $^{**}P \le 0.01$, $^{***}P \le 0.001$, or $^{****}P \le 0.0001$ by one-way ANOVA with Tukey's post hoc test; separate comparisons were made between conditions of each cell line.

and the α_2^{MED} β_1^{MED} MSCs for all the MSC lines (Fig. 7*E*). The unsorted, stained MSC lines had significantly less IDO activity relative to unsorted, unstained MSCs for all the MSC lines (Fig. 7*E*). These trends were similar for PD-L1 expression, as the $\alpha_V^{MED}\alpha_5^{MED}$ subpopulation had significantly greater PD-L1 expression relative to the $\alpha_V^{LO}\alpha_5^{LO}$ MSCs for all the MSC lines (Fig. 7*F*). The $\alpha_V^{HI}\alpha_5^{HI}$ subpopulation had significantly greater PD-L1 expression relative to the $\alpha_V^{LO}\alpha_5^{LO}$, $\alpha_V^{MED}\alpha_5^{MED}$, and unsorted, stained MSCs for all the MSC lines as well (Fig. 7*F*). The unsorted, stained MSC lines had significantly less PD-L1 expression relative to unsorted, unstained MSCs for two of the MSC lines (Fig. 7*F*).

Discussion

With the emergence of new biomaterial strategies to enhance the immunosuppressive function of MSCs (35) and ongoing clinical trials worldwide that utilize MSC–biomaterial combination products, there is an unmet need to characterize the functional heterogeneity of MSCs on biomaterials and develop cell sorting methods that may help reduce the heterogeneity of these combination products. Here, we demonstrated that the magnitude of immunosuppressive capacity of IFN-γ–licensed MSCs on biomaterials between donor cell lines correlated with IDO activity. For MSCs cultured on fibrin, the engagement of the α_V and α_5 integrin subunits enhanced IFN-γ–licensed MSC immunosuppressive capacity, while the engagement of the α_2 and β_1 integrin subunits enhanced IFN-γ–licensed MSC immunosuppressive capacity on collagen. The magnitude of expression of these integrin subunits on subpopulations of unlicensed MSCs correlated with the magnitude of IFN-γ–licensed MSC immunosuppressive capacity on their respective biomaterials. Sorting for MSCs that expressed high levels of integrin subunits specific to a biomaterial enriched for MSCs of greater immunosuppressive capacity with IFN-γ licensing than unsorted, stained MSCs. The role of other biomaterial factors contributing to IFN-γ–licensed MSC immunosuppressive capacity, such as the mechanical properties of the hydrogels, is outside the scope of this study.

While both PD-L1 expression and IDO activity were both strongly increased by IFN-γ licensing in MSCs, only IDO activity correlated with the immunosuppressive capacity of the IFN-γ–licensed MSCs between the donors on both fibrin and collagen hydrogels. Previous work has similarly shown that IFN-γ up-regulates IDO and PD-L1 expression in human bone marrow–derived MSCs cultured in vitro on TCPS (34) and RGD-modified PEG hydrogels (24), which share common integrin binding domains with fibrin (15, 36). Also, human bone marrow–derived MSCs cultured on collagen containing substrates demonstrated no deficiencies in up-regulating immune-related cytokines with IFN-γ stimulation compared to MSCs cultured on TCPS (37). Functionally, however, previous work has only shown that IDO activity regulates the ability of IFN-γ or IFN-γ/TNF-α–stimulated human bone marrow–derived MSCs to reduce the proliferation of T cells in vitro that were activated with anti-CD3/CD28 or in mixed lymphocyte reactions (28, 38). Furthermore, variations between human bone marrow–derived MSC donors in their ability to reduce T-cell proliferation in vitro significantly correlated with variations in IDO expression of the IFN-γ/TNF-α–stimulated MSCs cultured on TCPS (28). In contrast to the present study, other studies have demonstrated that PD-L1 up-regulation in mouse bone marrow–derived MSCs and human placenta–derived MSCs had a strong functional role in reducing T-cell proliferation (39, 40). These discrepancies, however, may be due to differences in cell and tissue source, as human bone marrow–derived MSCs were used in the present study.

The binding of the RGD integrin subunits α_V and α_5 was critical to the immunosuppressive capacity and cell morphology of IFN-γ–licensed MSCs on fibrin hydrogels; inhibiting binding of both integrins reduced this immunosuppressive capacity to the greatest extent compared to inhibiting either integrin alone. This was in part due to the ability of these integrins to regulate IDO activity and PD-L1 expression. The expression of IDO in TNF-α/IFN-γ–stimulated MSCs cultured in RGD-modified alginate hydrogels has previously been shown to depend on the bulk stiffness of the hydrogels (41); as integrin binding is one of the key mediators of the ability of cells to sense their mechanical environment (42), these findings may also support the hypothesis that binding to RGD moieties can regulate the immunosuppressive capacity of MSCs. Several studies have similarly demonstrated that binding of both $\alpha_V\beta_{3/5}$ and $\alpha_5\beta_1$ integrins is critical to the ability of cells to engage with fibrin and RGD-modified hydrogels. Inhibition of the spreading of smooth muscle cells and the ability of endothelial cells to form lumens in fibrin was similarly shown to depend on blocking both the $\alpha_V\beta_3$ and the $\alpha_5\beta_1$ integrins (43, 44). Furthermore, the ability of human bone marrow–derived MSCs to adhere to RGD-modified PEG gels was shown to depend on both the binding of $\alpha_V\beta_3$ and β_1 integrins (45). Thus, engagement of the RGD integrins, through fibrin or potentially any RGD ligand containing biomaterial, is critical to the ability of IFN-γ–licensed MSCs to immunosuppress on these substrates.

The binding of the collagen integrin subunits α_2 and β_1 was critical to the immunosuppressive capacity and cell morphology of IFN-γ–licensed MSCs on collagen I hydrogels, in part by their ability to regulate PD-L1 expression and IDO activity. The ability of human bone marrow–derived MSCs to adhere to GFOGER- (collagen I mimetic peptide) modified PEG gels was similarly shown to depend on α_2 integrin binding (45). The expression of several immunosuppressive genes in TNF-α/IFN-γ–pulsed MSCs cultured in collagen-alginate hydrogels was shown to depend on the stiffness and viscoelasticity of the hydrogels (46). As collagen I was the main substrate for these MSCs to engage with and integrins partly regulate the ability of cells to sense their mechanical microenvironment (42), these findings may also support the hypothesis that binding to collagen domains regulates the immunosuppressive capacity of MSCs. Human IFN-γ–licensed MSCs cultured on multilayers of collagen and heparin demonstrated higher expression of inflammatory cytokines relative to cells cultured on TCPS, suggesting that engagement of collagen integrins regulates MSC immunomodulation (37). In several readouts, blocking engagement of the β_1 subunit inhibited IFN-γ–licensed immunosuppressive capacity more than blocking the α_2 subunit alone; blocking both integrin subunits did not lead to a synergistic effect (Fig. 5). This may be due to the fact that blocking α_2 only blocks the $\alpha_2\beta_1$ integrin and that blocking β_1 blocks multiple β_1 containing collagen integrins ($\alpha_1\beta_1$, $\alpha_2\beta_1$, $\alpha_{10}\beta_1$, and $\alpha_{11}\beta_1$). This finding is supported by the fact that engagement of both $\alpha_2\beta_1$ and $\alpha_{11}\beta_1$ to collagen I was critical for the survival of human bone marrow–derived MSCs (47).

The immunosuppressive capacity and cell morphology of IFN-γ–licensed MSCs cultured on TCPS depended strongly on binding of the integrin subunit α_V and less so on binding of the α_5 subunit. Previous work has demonstrated that the adhesion proteins fibronectin, which binds to the $\alpha_5\beta_1$ integrin, and vitronectin, which binds to the $\alpha_V\beta_5$ integrin, contained in serum adsorb to the surface of TCPS (36, 48). However, the adhesion and spreading of adherent cells, such as endothelial cells and fibroblasts, on TCPS have been shown to be more strongly dependent on serum-derived vitronectin adsorption to TCPS than adsorption of serum-derived fibronectin (36, 49). This is potentially due to the fact that fibronectin binds to TCPS at suboptimal concentrations relative to other culture substrates (49).

The amount of integrin expression on unlicensed MSCs specific to each biomaterial (α_V/ α_5 for fibrin and TCPS and α_2/β_1 for collagen) predicted the magnitude of IFN-γ–licensed MSC immunosuppressive capacity in subpopulations within each donor. Furthermore, the amount of surface integrin expression also predicted the magnitude of IDO activity and PD-L1 expression. Previous work has demonstrated that the morphology of IFN-γ–stimulated human bone

marrow–derived MSC subpopulations can be used to predict the immunosuppressive capacity of MSCs (32). As the morphology of MSCs and their ability to spread depends on their integrin binding (50), these findings may also support the fact that integrin expression regulates the degree to which subpopulations of IFN-γ–licensed MSCs can immunosuppress. Other studies have supported the notion of the existence of subpopulations of MSCs within donors that have higher differentiation potential and paracrine effects based on their cell size (51, 52). Furthermore, previous work has demonstrated that overexpression of the α_5 integrin subunit in MSCs led to greater osteogenic differentiation (53), supporting the premise that the magnitude of integrin surface expression in MSCs can regulate their phenotype.

MSCs that demonstrated high expression of integrins specific to each biomaterial exhibited greater IFN-γ–licensed immunosuppressive capacity than unsorted, stained cells; however, unsorted, unstained cells exhibited greater immunosuppressive capacity than unsorted, stained cells. While the α_V, α_5, α_2, and β_1 integrin subunit antibodies utilized for FACS sorting have no reported functional blocking of integrin binding and demonstrated no observable inhibition of cell spreading, we hypothesize that these antibodies inhibit integrin binding to their respective ligands to a certain extent, as has been previously demonstrated with other integrin antibodies (54, 55), and therefore reduce MSC immunosuppressive capacity. With technologies that enable removal of antibody fluorochrome conjugates (56) (which are currently not commercially available for the tested human antibodies in this paper at this time), we hypothesize that sorting MSCs by the magnitude of their integrin expression specific to a biomaterial may provide a generalizable way to enrich for MSCs of greater immunosuppressive capacity than unsorted MSCs for MSC–biomaterial combination therapies.

Although the magnitude of integrin expression predicted the immunosuppressive capacity of IFN-γ–licensed MSC subpopulations on biomaterials, it did not predict variations in immunosuppressive capacity between donor cell lines. Previous work has demonstrated that the morphology of IFN-γ–stimulated human bone marrow–derived MSCs predicts donor-to-donor variations in immunosuppressive capacity of unlicensed and IFN-γ–licensed MSCs; however, these correlations varied between MSCs manufactured under different conditions (31). Furthermore, multiple factors, both intrinsic and introduced during the manufacturing process, likely contribute to donor-to-donor variations in MSC immunosuppressive capacity, such as donor age, gender, genetic background, surface marker expression, and in vitro population doubling time, which have previously been shown to contribute to donor-to-donor MSC functional heterogeneity (57–59). Evaluating the combination of these factors, in addition to integrin expression, may lead to improved methods of predicting donor-to-donor variations in MSC immunosuppressive capacity.

The results of this study demonstrate that integrin surface expression specific to fibrin and collagen biomaterials, as well as integrin engagement, predict and/or influence the magnitude of IFN-γ–licensed MSC immunosuppressive capacity. We hypothesize that sorting MSCs by the amount of integrin expression specific to any biomaterial (natural or engineered synthetic) may provide a generalizable way for identifying subpopulations of MSCs of varying IFN-γ–licensed immunosuppressive capacity. Furthermore, these findings may lead to methods of manufacturing MSCs for MSC–biomaterial combination products that can enrich for MSC subpopulations with high immunosuppressive capacity and potentially improve the efficacy and clinical success of these products. Identifying MSCs of varying immunosuppressive capacity by the magnitude of integrin expression may help enhance product characterization for MSC–biomaterial combination and may help minimize heterogeneity introduced by MSC manufacturing processes. As other MSC reparative functions, such as their ability to differentiate into bone and their secretory capacity, have also been shown to depend on integrin binding to biomaterials (45, 60), the magnitude of integrin expression on MSCs may more broadly identify MSCs of potentially varying therapeutic capacities on biomaterials as well.

Methods

MSC Manufacturing and Expansion. Human bone marrow–derived stromal cells from RoosterBio (see Fig. 1*A* for donor specifications) were expanded as previously described (31). Briefly, MSCs were grown in RoosterBio expansion medium at an initial plating density of ∼3,700 cells per square centimeter in a T175 tissue culture flask. Upon reaching ∼80% confluency, cells were trypsinized and reseeded at ∼3,700 cells per square centimeter, designated as one passage. Cells were continuously expanded with no freezing or thawing between passages, with fractions of cells being frozen during expansion at passages 2 through 5. All MSC cells were obtained from patients with the proper consent.

Human bone marrow–derived stromal cells from AllCells and Lonza were expanded as previously described (31). Briefly, MSCs were cultured in Minimum Essential Medium α (α-MEM) media (Gibco, Catalog No. 12571) supplemented with 16% fetal bovine serum (FBS), 1% Penicillin-Streptomycin (P/S), and L-glutamine at an initial seeding density of 60 cells per square centimeter in a T175 flask. Upon reaching ∼80% confluence, cells were trypsinized and reseeded at 60 cells per square centimeter in a T175 flask, designated as one passage. Cells were continuously expanded with no freezing or thawing between passages, with fractions of cells being frozen during expansion at passages 3, 5, and 7. All MSC cells were obtained from patients with the proper consent.

Fibrin and Collagen Gel Preparation. For all experiments, 50 μL fibrin or collagen hydrogel was prepared in a 96-well flat-bottomed tissue culture plate. For preparation of fibrin gels, bovine fibrinogen (Sigma, Catalog No. F8630) was reconstituted in phosphate buffered saline (PBS) at a concentration of 7.5 mg/mL clottable protein and sterile filtered. A total of 40 μL fibrinogen solution was then mixed with 10 μL 5 U/mL bovine thrombin solution (Sigma, Catalog No. T4648) in PBS and was then cross-linked for at least 30 min at 37 °C, yielding a fibrin hydrogel at 6 mg/mL fibrinogen and 1 U/mL thrombin. For preparation of collagen gels, a 6-mg/mL collagen I gel was prepared by mixing high-concentration rat tail collagen I (Corning, Catalog No. 354249), 10× PBS (1/10 final volume), 1 N sodium hydroxide (0.0023 × volume of collagen added), and distilled water on ice. A total of 50 μL resulting collagen solution was dispensed into the well and was cross-linked for 30 min at 37 °C.

Mechanical Characterization of Hydrogels. The mechanical properties of the hydrogels were measured using an Anton Paar MCR302 rheometer equipped with an 8-mm parallel-plate setting. The hydrogels with a thickness of 1 mm were in situ formed between the plates at 37 °C for 30 min. For oscillatory time sweep experiments, the constant strain and frequency were fixed at 1% and 1 Hz, respectively.

MSC Culture with Hydrogels. Prior to seeding MSCs onto hydrogels, 1×10^6 frozen, passage 2 to 5 MSCs were seeded into a T175 flask in α-MEM media (Gibco, Catalog No. 12571) supplemented with 16% FBS, 1% P/S, and L-glutamine. After 2 d of culture, MSCs were removed with TrypLE express enzyme (Gibco, Catalog No. 12604) and were seeded on top of fibrin or collagen hydrogels at a concentration of 10,000 cells per well. To remove MSCs adhered to the hydrogels, MSCs on fibrin gels were incubated in 0.25% Trypsin-ethylenediaminetetraacetic acid (EDTA) (Gibo, Catalog No. 25200) for 30 min at 37 °C, and MSCs on collagen gels were incubated in 200 U/mL collagenase type II (Gibco, Catalog No. 17101015) for 30 min at 37 °C. The morphology of the MSCs was assessed by fixing the cells with 4% paraformaldehyde, staining the cells with DAPI (Thermo Fisher Scientific, Catalog No. 62488) and Texas Red-X Phalloidin (Thermo Fisher Scientific, Catalog No. T7471) according to manufacturer's protocols and imaging the cells on an EVOS fluorescence microscope.

PBMC Immunosuppression Assay. After overnight culture with hydrogels, MSCs were activated for 24 h in complete α-MEM media either in the presence or absence of 50 ng/mL IFN-γ. Following activation, the MSCs were washed twice with PBS and then cultured in RPMI1640 media (Gibco, Catalog No. 11875) supplemented with 10% FBS and 1% P/S. A total of 1×10^5 PBMCs stained with CFSE (Invitrogen, Catalog No. C34554) were cultured on top of the MSCs in the presence of 1×10^5 Dynabeads Human T-Activator CD3/CD28 (Gibco, Catalog No. 11131D) and 30 ng/mL human IL-2 (Peprotech, Catalog No. 200-02). After 3 d of coculture, the PBMCs were removed from

the hydrogels and analyzed by flow cytometry (Fig. 1*B*). PBMCs were removed from fibrin gels by vigorous pipetting and were removed from collagen gels by incubation in 200 U/mL collagenase type II for 30 min at 37 °C. PBMCs were stained with the following antibodies (manufacturer, clone name, and fluorophore in parenthesis): anti-CD3 [BioLegend, HIT3a, phycoerythrin (PE)], anti-CD4 (BioLegend, OKT4, PE/Cy7), anti-CD8 (BioLegend, RPA-T8, APC), and anti-CD25 (BioLegend, M-A251, Pacific Blue). Live cells were determined with the Zombie NIR Fixable Viability Kit (BioLegend, Catalog No. 423105). Samples were run on a BD LSRFortessa X-20 flow cytometer. The percentage of proliferating and activated T cells was analyzed on FlowJo version 10 (*SI Appendix*, Fig. S1) and normalized to control PBMCs with hydrogel alone (no MSCs).

IDO Activity and PD-L1 Expression Assay. Following activation with and without IFN-γ in complete α-MEM media, MSCs were cultured in fresh, complete RPMI1640 media. After 24 h, the conditioned media was collected and subsequently analyzed for kynurenine concentration using the Kynurenine Competitive Enzyme Immunoassay (IBL America, Catalog No. IB89190) according to the manufacturer's protocol. The MSCs were also collected and analyzed for PD-L1 expression with flow cytometry analysis on a BD LSRFortessa X-20 flow cytometer. Collected MSCs were stained with anti–PD-L1 antibody (BioLegend, 29E.2A3, APC). Live cells were determined with the Zombie NIR Fixable Viability Kit (BioLegend, Catalog No. 423105).

Integrin Blocking Assay. Prior to seeding MSCs onto hydrogels, MSCs were preincubated with the following reagents or antibodies at the following concentrations for 30 min at 37 °C: 10 μM cilengitide (α_V blocker [R&D, Catalog No. 5870]), 10 μg/mL anti-$\alpha_5\beta_1$ (Millipore, Catalog No. MABT820, Rat IgG2a isotype), 10 μg/mL Rat IgG2a isotype control (Millipore, Catalog No. MABF1077Z), 10 μg/mL anti-α_2 (BioLegend, Catalog No. 359304, Ms IgG1-κ isotype), 10 μg/mL anti-β_1 (BioLegend, Catalog No. 921304, Mouse IgG1-κ isotype), and/or 10 μg/mL or 20 μg/mL Mouse IgG1-κ isotype control antibody (BioLegend, Catalog No. 400153). For the PBMC immunosuppression assay, the same concentration of antibodies was added to the media with the MSCs during overnight incubation with the hydrogel and during the 24-h activation period with IFN-γ; the antibodies were removed and washed off with PBS with the addition of the PBMCs. For the IDO activity and PD-L1 expression assay, the same concentration of antibodies was added to the media for the entire length of the experiment.

Integrin FACS Staining and Sorting. Prior to FACS sorting MSCs, 5×10^5 frozen, passage 2 to 5 MSCs were seeded into a T175 flask in α-MEM (Gibco, Catalog No. 12571) supplemented with 16% FBS, 1% P/S, and L-glutamine. After 2 to 5 d of culture, MSCs were removed with TrypLE express enzyme and were stained with the following antibodies in FACS staining buffer (PBS with 2% FBS and 1% P/S): anti-α_V antibody [R&D Systems, P2W7, fluorescein isothiocyanate (FITC)], anti-α_5 antibody (BD Biosciences, IIA1, PE), anti- α_2 antibody (eBioscience, Y418, FITC), and/or anti-β_1 antibody (BD Biosciences, MAR4, PE). MSCs were then FACS sorted based on the magnitude of their expression of their integrins in FACS sorting buffer (PBS with 0.5% BSA, 2 mM EDTA, and 1% P/S) with a BD FACSAria Fusion Cell Sorter, a BD FACSAria II, or a BD FACSAria III. Unsorted stained and unstained MSCs underwent the same incubations and centrifugation spins in the FACS staining and FACS sorting buffers to account for the negative impact of these treatments on the cells.

Statistics. All values in the present study are expressed as means ± SD. Data were statistically analyzed in GraphPad Prism 7 (GraphPad Software Inc.). Significance between groups was determined using ANOVAs with Tukey's post hoc test. Significance of correlations was determined using a two-tailed Spearman's rank correlation. Statistical significance was determined at $P < 0.05$.

Data Availability. All study data are included in the article and/or *SI Appendix*. Raw data have been deposited in the Open Science Framework (https://osf.io/b85da/).

ACKNOWLEDGMENTS. We thank Steven R. Bauer for useful discussions. We also thank Matthew Klinker, Elizabeth Lessey-Morillon, Carolyn Laurencot, and Raj Puri for their review of this manuscript. This work was supported in part by B.J.K.'s appointment to the Research Participation Program at the Center for Biologics Evaluation and Research administered by the Oak Ridge Institute for Science and Education through the US Department of Education and US FDA. This work was partially supported by research funds from the Division of Cellular and Gene Therapies. This work was also partially supported by the FDA of the US Department of Health and Human Services (HHS) as part of a financial assistance award (Center of Excellence in Regulatory Science and Innovation Grant to Johns Hopkins University, Grant No. U01FD005942) totaling $82,735 with 100% funded by the FDA/HHS. The contents are those of the author(s) and do not necessarily represent the official views of, nor an endorsement by, the FDA/HHS or the US Government.

1. Y. Wang, X. Chen, W. Cao, Y. Shi, Plasticity of mesenchymal stem cells in immunomodulation: pathological and therapeutic implications. *Nat. Immunol.* **15**, 1009–1016 (2014).
2. B. J. Jones, S. J. McTaggart, Immunosuppression by mesenchymal stromal cells: from culture to clinic. *Exp. Hematol.* **36**, 733–741 (2008).
3. T. Squillaro, G. Peluso, U. Galderisi, Clinical trials with mesenchymal stem cells: an update. *Cell Transplant.* **25**, 829–848 (2016).
4. D. Mougiakakos *et al*., The impact of inflammatory licensing on heme oxygenase-1-mediated induction of regulatory T cells by human mesenchymal stem cells. *Blood* **117**, 4826–4835 (2011).
5. G. Ren *et al*., Mesenchymal stem cell-mediated immunosuppression occurs via concerted action of chemokines and nitric oxide. *Cell Stem Cell* **2**, 141–150 (2008).
6. D. Polchert *et al*., IFN-γ activation of mesenchymal stem cells for treatment and prevention of graft versus host disease. *Eur. J. Immunol.* **38**, 1745–1755 (2008).
7. E. Gonzalez-Rey *et al*., Human adult stem cells derived from adipose tissue protect against experimental colitis and sepsis. *Gut* **58**, 929–939 (2009).
8. E. Zappia *et al*., Mesenchymal stem cells ameliorate experimental autoimmune encephalomyelitis inducing T-cell anergy. *Blood* **106**, 1755–1761 (2005).
9. O. Levy *et al*., Shattering barriers toward clinically meaningful MSC therapies. *Sci. Adv.* **6**, eaba6884 (2020).
10. G. Moll *et al*., MSC therapies for COVID-19: Importance of patient coagulopathy, thromboprophylaxis, cell product quality and mode of delivery for treatment safety and efficacy. *Front. Immunol.* **11**, 1091 (2020).
11. D. G. Phinney, Functional heterogeneity of mesenchymal stem cells: implications for cell therapy. *J. Cell. Biochem.* **113**, 2806–2812 (2012).
12. A. Kurtz, Mesenchymal stem cell delivery routes and fate. *Int. J. Stem Cells* **1**, 1–7 (2008).
13. M. O. Dellacherie, B. R. Seo, D. M. Mooney, Macroscale biomaterials strategies for local immunomodulation. *Nat. Rev. Mater.* **4**, 379–397 (2019).
14. R. S. Tuan, G. Boland, R. Tuli, Adult mesenchymal stem cells and cell-based tissue engineering. *Arthritis Res. Ther.* **5**, 32–45 (2003).
15. M. Barczyk, S. Carracedo, D. Gullberg, Integrins. *Cell Tissue Res.* **339**, 269–280 (2010).
16. D. Docheva, C. Popov, W. Mutschler, M. Schieker, Human mesenchymal stem cells in contact with their environment: surface characteristics and the integrin system. *J. Cell. Mol. Med.* **11**, 21–38 (2007).
17. A. J. García, Get a grip: Integrins in cell-biomaterial interactions. *Biomaterials* **26**, 7525–7529 (2005).
18. J. R. Mauney, V. Volloch, D. L. Kaplan, Role of adult mesenchymal stem cells in bone tissue engineering applications: Current status and future prospects. *Tissue Eng.* **11**, 787–802 (2005).
19. A. R. Tan, C. T. Hung, Concise review: Mesenchymal stem cells for functional cartilage tissue engineering: Taking cues from chondrocyte-based constructs. *Stem Cells Transl. Med.* **6**, 1295–1303 (2017).
20. T. H. Qazi, D. J. Mooney, G. N. Duda, S. Geissler, Biomaterials that promote cell-cell interactions enhance the paracrine function of MSCs. *Biomaterials* **140**, 103–114 (2017).
21. M. Pumberger *et al*., Synthetic niche to modulate regenerative potential of MSCs and enhance skeletal muscle regeneration. *Biomaterials* **99**, 95–108 (2016).
22. V. Bunpetch *et al*., Strategies for MSC expansion and MSC-based microtissue for bone regeneration. *Biomaterials* **196**, 67–79 (2019).
23. V. V. Rao, M. K. Vu, H. Ma, A. R. Killaars, K. S. Anseth, Rescuing mesenchymal stem cell regenerative properties on hydrogel substrates post serial expansion. *Bioeng. Transl. Med.* **4**, 51–60 (2018).
24. J. R. García *et al*., IFN-γ-tethered hydrogels enhance mesenchymal stem cell-based immunomodulation and promote tissue repair. *Biomaterials* **220**, 119403 (2019).
25. A. S. Mao *et al*., Programmable microencapsulation for enhanced mesenchymal stem cell persistence and immunomodulation. *Proc. Natl. Acad. Sci. U.S.A.* **116**, 15392–15397 (2019).
26. A. Gonzalez-Pujana *et al*., Multifunctional biomimetic hydrogel systems to boost the immunomodulatory potential of mesenchymal stromal cells. *Biomaterials* **257**, 120266 (2020).
27. R. A. Marklein, J. Lam, M. Guvendiren, K. E. Sung, S. R. Bauer, Functionally-relevant morphological profiling: A tool to assess cellular heterogeneity. *Trends Biotechnol.* **36**, 105–118 (2018).
28. M. François, R. Romieu-Mourez, M. Li, J. Galipeau, Human MSC suppression correlates with cytokine induction of indoleamine 2,3-dioxygenase and bystander M2 macrophage differentiation. *Mol. Ther.* **20**, 187–195 (2012).
29. R. H. Lee *et al*., TSG-6 as a biomarker to predict efficacy of human mesenchymal stem/progenitor cells (hMSCs) in modulating sterile inflammation in vivo. *Proc. Natl. Acad. Sci. U.S.A.* **111**, 16766–16771 (2014).
30. D. J. Kota *et al*., Prostaglandin E2 indicates therapeutic efficacy of mesenchymal stem cells in experimental traumatic brain injury. *Stem Cells* **35**, 1416–1430 (2017).
31. M. W. Klinker, R. A. Marklein, J. L. Lo Surdo, C.-H. Wei, S. R. Bauer, Morphological features of IFN-γ-stimulated mesenchymal stromal cells predict overall immunosuppressive capacity. *Proc. Natl. Acad. Sci. U.S.A.* **114**, E2598–E2607 (2017).

32. R. A. Marklein *et al*., Morphological profiling using machine learning reveals emergent subpopulations of interferon-γ-stimulated mesenchymal stromal cells that predict immunosuppression. *Cytotherapy* **21**, 17–31 (2019).
33. Z. X. Yang *et al*., CD106 identifies a subpopulation of mesenchymal stem cells with unique immunomodulatory properties. *PLoS One* **8**, e59354 (2013).
34. H. M. Wobma *et al*., Dual IFN-γ/hypoxia priming enhances immunosuppression of mesenchymal stromal cells through regulatory proteins and metabolic mechanisms. *J. Immunol. Regen. Med.* **1**, 45–56 (2018).
35. Y. Chen, Z. Shu, K. Qian, J. Wang, H. Zhu, Harnessing the properties of biomaterial to enhance the immunomodulation of mesenchymal stem cells. *Tissue Eng. Part B Rev.* **25**, 492–499 (2019).
36. J. G. Steele, G. Johnson, P. A. Underwood, Role of serum vitronectin and fibronectin in adhesion of fibroblasts following seeding onto tissue culture polystyrene. *J. Biomed. Mater. Res.* **26**, 861–884 (1992).
37. D. A. Castilla-Casadiego, J. R. García, A. J. García, J. Almodovar, Heparin/collagen coatings improve human mesenchymal stromal cell response to interferon gamma. *ACS Biomater. Sci. Eng.* **5**, 2793–2803 (2019).
38. R. Meisel *et al*., Human bone marrow stromal cells inhibit allogeneic T-cell responses by indoleamine 2,3-dioxygenase-mediated tryptophan degradation. *Blood* **103**, 4619–4621 (2004).
39. H. Sheng *et al*., A critical role of IFNgamma in priming MSC-mediated suppression of T cell proliferation through up-regulation of B7-H1. *Cell Res.* **18**, 846–857 (2008).
40. Y. Z. Gu *et al*., Different roles of PD-L1 and FasL in immunomodulation mediated by human placenta-derived mesenchymal stem cells. *Hum. Immunol.* **74**, 267–276 (2013).
41. M. Darnell, L. Gu, D. Mooney, RNA-seq reveals diverse effects of substrate stiffness on mesenchymal stem cells. *Biomaterials* **181**, 182–188 (2018).
42. K. H. Vining, D. J. Mooney, Mechanical forces direct stem cell behaviour in development and regeneration. *Nat. Rev. Mol. Cell Biol.* **18**, 728–742 (2017).
43. Y. Ikari, K. O. Yee, S. M. Schwartz, Role of α5β1 and alphavbeta3 integrins on smooth muscle cell spreading and migration in fibrin gels. *Thromb. Haemost.* **84**, 701–705 (2000).
44. K. J. Bayless, R. Salazar, G. E. Davis, RGD-dependent vacuolation and lumen formation observed during endothelial cell morphogenesis in three-dimensional fibrin matrices involves the α(v)β(3) and α(5)β(1) integrins. *Am. J. Pathol.* **156**, 1673–1683 (2000).
45. A. Y. Clark *et al*., Integrin-specific hydrogels modulate transplanted human bone marrow-derived mesenchymal stem cell survival, engraftment, and reparative activities. *Nat. Commun.* **11**, 114 (2020).
46. K. H. Vining, A. Stafford, D. J. Mooney, Sequential modes of crosslinking tune viscoelasticity of cell-instructive hydrogels. *Biomaterials* **188**, 187–197 (2019).
47. C. Popov *et al*., Integrins α2β1 and α11β1 regulate the survival of mesenchymal stem cells on collagen I. *Cell Death Dis.* **2**, e186 (2011).
48. S. R. Braam *et al*., Recombinant vitronectin is a functionally defined substrate that supports human embryonic stem cell self-renewal via alphavbeta5 integrin. *Stem Cells* **26**, 2257–2265 (2008).
49. J. G. Steele, B. A. Dalton, G. Johnson, P. A. Underwood, Adsorption of fibronectin and vitronectin onto Primaria and tissue culture polystyrene and relationship to the mechanism of initial attachment of human vein endothelial cells and BHK-21 fibroblasts. *Biomaterials* **16**, 1057–1067 (1995).
50. E. A. Cavalcanti-Adam *et al*., Cell spreading and focal adhesion dynamics are regulated by spacing of integrin ligands. *Biophys. J.* **92**, 2964–2974 (2007).
51. L. Yin *et al*., Label-free separation of mesenchymal stem cell subpopulations with distinct differentiation potencies and paracrine effects. *Biomaterials* **240**, 119881 (2020).
52. Z. Poon *et al*., Bone marrow regeneration promoted by biophysically sorted osteoprogenitors from mesenchymal stromal cells. *Stem Cells Transl. Med.* **4**, 56–65 (2015).
53. Z. Hamidouche *et al*., Priming integrin α5 promotes human mesenchymal stromal cell osteoblast differentiation and osteogenesis. *Proc. Natl. Acad. Sci. U.S.A.* **106**, 18587–18591 (2009).
54. S. Fujita, H. Suzuki, M. Kinoshita, S. Hirohashi, Inhibition of cell attachment, invasion and metastasis of human carcinoma cells by anti-integrin β 1 subunit antibody. *Jpn. J. Cancer Res.* **83**, 1317–1326 (1992).
55. F. J. Fogerty, S. K. Akiyama, K. M. Yamada, D. F. Mosher, Inhibition of binding of fibronectin to matrix assembly sites by anti-integrin (alpha 5 beta 1) antibodies. *J. Cell Biol.* **111**, 699–708 (1990).
56. J. Pankratz *et al*., REAlease technology: Controlled release of antibody-fluorochrome conjugates for maximal flexibility in flow sorting and fluorescence microscopy applications. *Cancer Res.* **79**, 10.1158/1538-7445.AM2019-4048 (2019).
57. G. Siegel *et al*., Phenotype, donor age and gender affect function of human bone marrow-derived mesenchymal stromal cells. *BMC Med.* **11**, 146 (2013).
58. T. Wang, J. Zhang, J. Liao, F. Zhang, G. Zhou, Donor genetic backgrounds contribute to the functional heterogeneity of stem cells and clinical outcomes. *Stem Cells Transl. Med.* **9**, 1495–1499 (2020).
59. O. Katsara *et al*., Effects of donor age, gender, and in vitro cellular aging on the phenotypic, functional, and molecular characteristics of mouse bone marrow-derived mesenchymal stem cells. *Stem Cells Dev.* **20**, 1549–1561 (2011).
60. N. Huebsch *et al*., Harnessing traction-mediated manipulation of the cell/matrix interface to control stem-cell fate. *Nat. Mater.* **9**, 518–526 (2010).